



Numerical simulation of blood flow in a straight artery under the influence of magnetic field

G. C. Shit, A. Sinha, A. Mondal, S. Majee

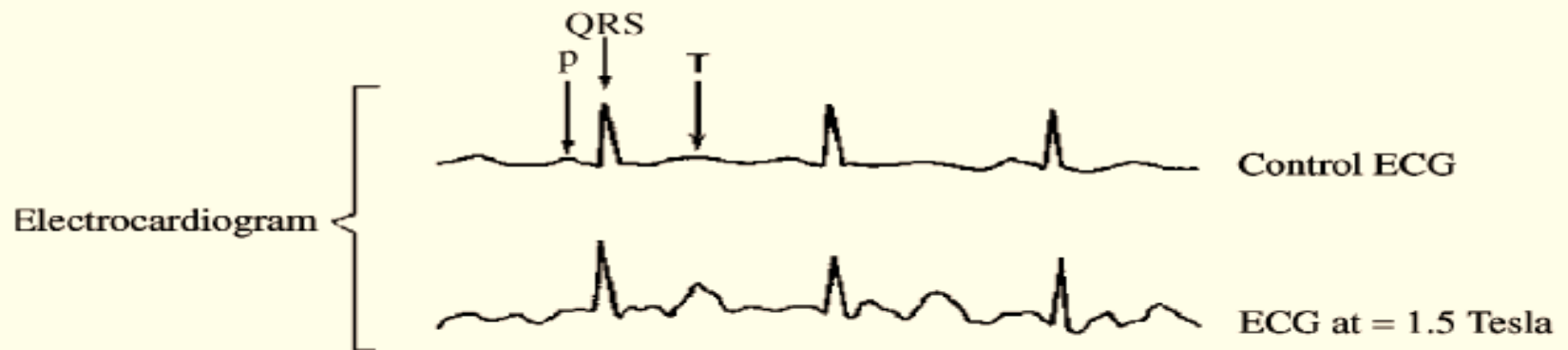
***Department of Mathematics
Jadavpur University, Kolkata***

**COMSOL
CONFERENCE
2014 BANGALORE**

Excerpt from the Proceedings of the 2014 COMSOL Conference in Bangalore

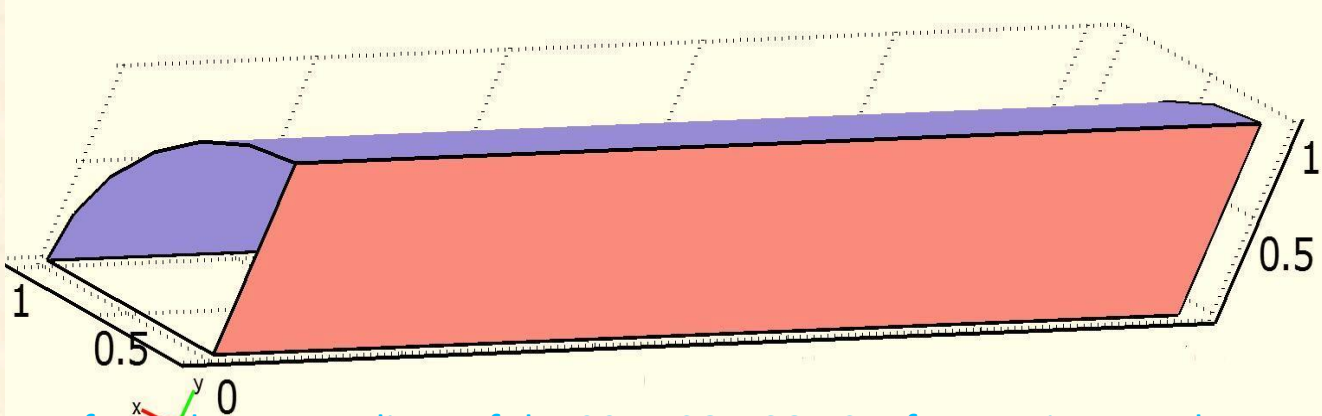
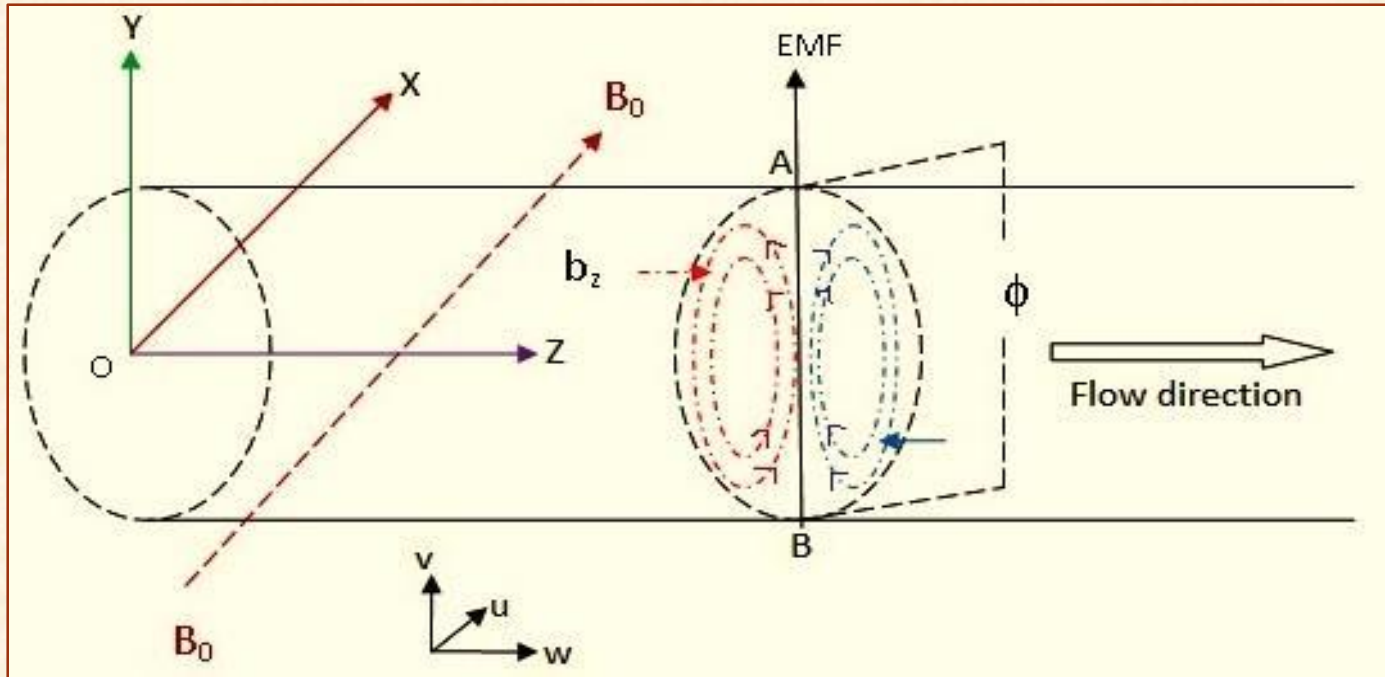
Motivation

- Interaction of magnetic field with the flow of electrically conducting fluid (blood)
- Downstream Singularities in the cardiovascular system
- Application to Magnetic Resonance Imaging (MRI)
- Effect of magnetic field on the T wave in ECG



Tenforde, T.S., *Progress in Biophysics & Molecular Biology*, 87(2005) 279

Representation of elementary volume



Excerpt from the Proceedings of the 2014 COMSOL Conference in Bangalore

Governing Equations

The basic governing equations for magnetohydrodynamic (MHD) fluid flow are

$$\vec{\nabla}' \cdot \vec{V}' = 0$$

$$\rho \left(\frac{\partial \vec{V}'}{\partial t'} + (\vec{V}' \cdot \vec{\nabla}') \vec{V}' \right) = -\vec{\nabla}' p' + \eta \vec{\nabla}'^2 \vec{V}' + \vec{J}' \times \vec{B}'$$

The Maxwell's equations of electromagnetism

$$\vec{\nabla}' \cdot \vec{E}' = \frac{\rho_e}{\epsilon}$$

$$\vec{\nabla}' \times \vec{E}' = -\frac{\partial \vec{B}'}{\partial t'}$$

$$\vec{\nabla}' \times \vec{B}' = \mu_e \vec{J}'$$

$$\vec{\nabla}' \cdot \vec{B}' = 0$$

and the Ohm's law

$$\vec{J}' = \sigma [\vec{E}' + \vec{V}' \times \vec{B}']$$

Normalized Equations & characteristics parameters

Length	Velocity	Stress & Pressure	Time	Magnetic field	Induced current
a	V_0	ρV_0^2	$\frac{1}{\omega}$	$\frac{1}{a} \sqrt{\frac{\eta}{\sigma}}$	$\frac{1}{\mu_e a^2} \sqrt{\frac{\eta}{\sigma}}$

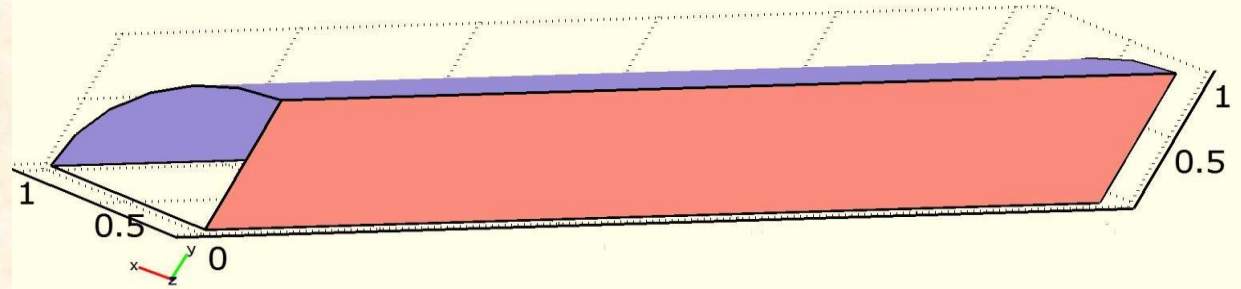
$$\vec{\nabla} \cdot \vec{V} = 0$$

$$\frac{\alpha^2}{Re} \frac{\partial \vec{V}}{\partial t} + (\vec{V} \cdot \vec{\nabla}) \vec{V} = -\vec{\nabla} p + \frac{1}{Re} \vec{\nabla}^2 \vec{V} + \frac{Ha}{Re R_m} (\vec{\nabla} \times \vec{b}) \times \hat{i} + \frac{1}{Re R_m} (\vec{\nabla} \times \vec{b}) \times \vec{b}$$

$$\frac{\alpha^2}{Re} \frac{\partial \vec{b}}{\partial t} + (\vec{V} \cdot \vec{\nabla}) \vec{b} = (\vec{b} \cdot \nabla) \vec{V} + Ha (\hat{i} \cdot \vec{\nabla}) \vec{V} + \frac{1}{R_m} \vec{\nabla}^2 \vec{b}$$

Reynolds number	Hartmann number	Magnetic Reynolds number	Womersley parameter
$Re = \frac{\rho a V_0}{\eta}$	$Ha = B_0 a \sqrt{\frac{\sigma}{\eta}}$	$R_m = a V_0 \mu_e \sigma$	$\alpha = a \sqrt{\frac{\omega}{\nu}}$

Boundary conditions



Inlet	Wall	Plane of symmetry (XOZ-plane)	Plane of symmetry (YOZ-plane)	Outlet
$w = \left[1 + \sin\left(t + \frac{3\pi}{2}\right) \right]$ $u = v = 0;$	$u = v = 0,$ $w = 0;$	$(\hat{n} \cdot \vec{\nabla})\vec{V} = \vec{0};$	$(\hat{n} \cdot \vec{\nabla})\vec{V} = \vec{0};$	$p = 0;$
$(\hat{n} \cdot \vec{\nabla})\vec{b} = \vec{0}$	$\vec{b} = \vec{0}$	$(\hat{n} \cdot \vec{\nabla})\vec{b} = \vec{0}$	$\vec{b} = \vec{0}$	$(\hat{n} \cdot \vec{\nabla})\vec{b} = \vec{0}$

Numerical methods and Mesh refinements

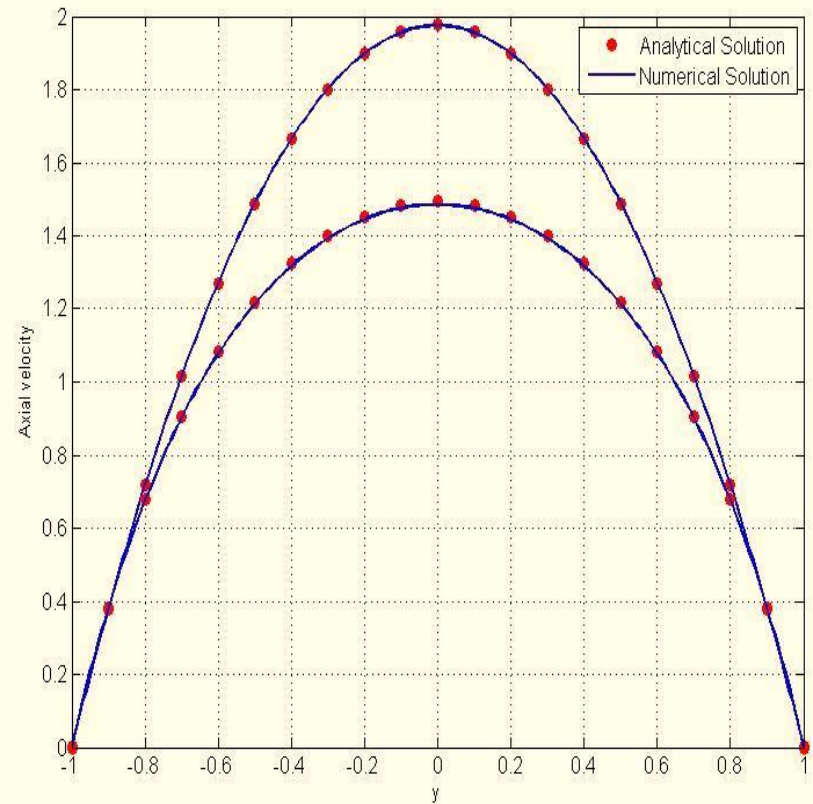
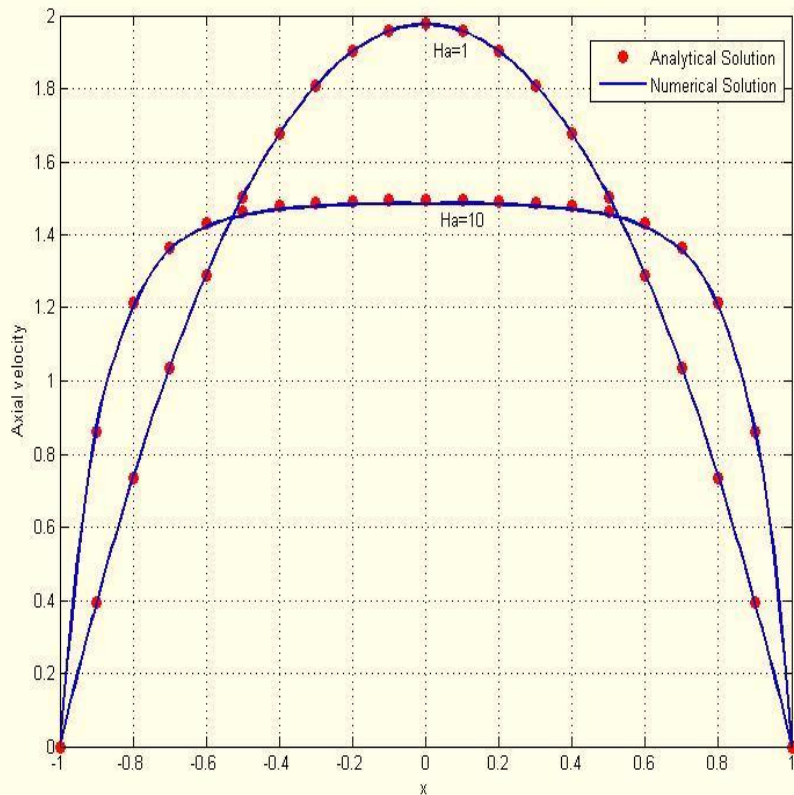
- Direct numerical simulation were performed with Comsol Multiphysics software®
- Mesh statistics for the Quarter part of the tube

Cases	Maximum Element Size (ES)	Number of Elements (NE)	No. of Degrees of freedom (DOF)	Number of triangular element at the entry section	Number of triangular element at the surface of the vessel wall
Case-I	0.30	46568	466982	38	6528
Case-II	0.20	163594	1538336	80	13486
Case-III	0.18	226680	2102756	89	17366
Case-IV	0.15	394192	3577693	125	25696

Absolute error in the axial velocity $w(x, 0.5, 90)$ for four different cases when $Re=300$

	$Ha=2$			$Ha=10$		
x	Case-I & Case-II	Case-II & Case-III	Case-III & Case-IV	Case-I & Case-II	Case-II & Case-III	Case-III & Case-IV
0.0	5×10^{-5}	4×10^{-5}	1×10^{-5}	5×10^{-3}	4×10^{-5}	1×10^{-5}
0.2	2×10^{-4}	4×10^{-5}	2×10^{-5}	3×10^{-3}	5×10^{-6}	3×10^{-6}
0.4	3×10^{-4}	6×10^{-5}	1×10^{-5}	1×10^{-3}	2×10^{-4}	1×10^{-5}
0.5	2×10^{-4}	6×10^{-5}	1×10^{-5}	4×10^{-3}	9×10^{-4}	4×10^{-5}
0.6	8×10^{-5}	1×10^{-5}	3×10^{-5}	1×10^{-2}	1×10^{-3}	1×10^{-4}
0.8	6×10^{-4}	8×10^{-5}	3×10^{-5}	8×10^{-3}	1×10^{-3}	2×10^{-4}

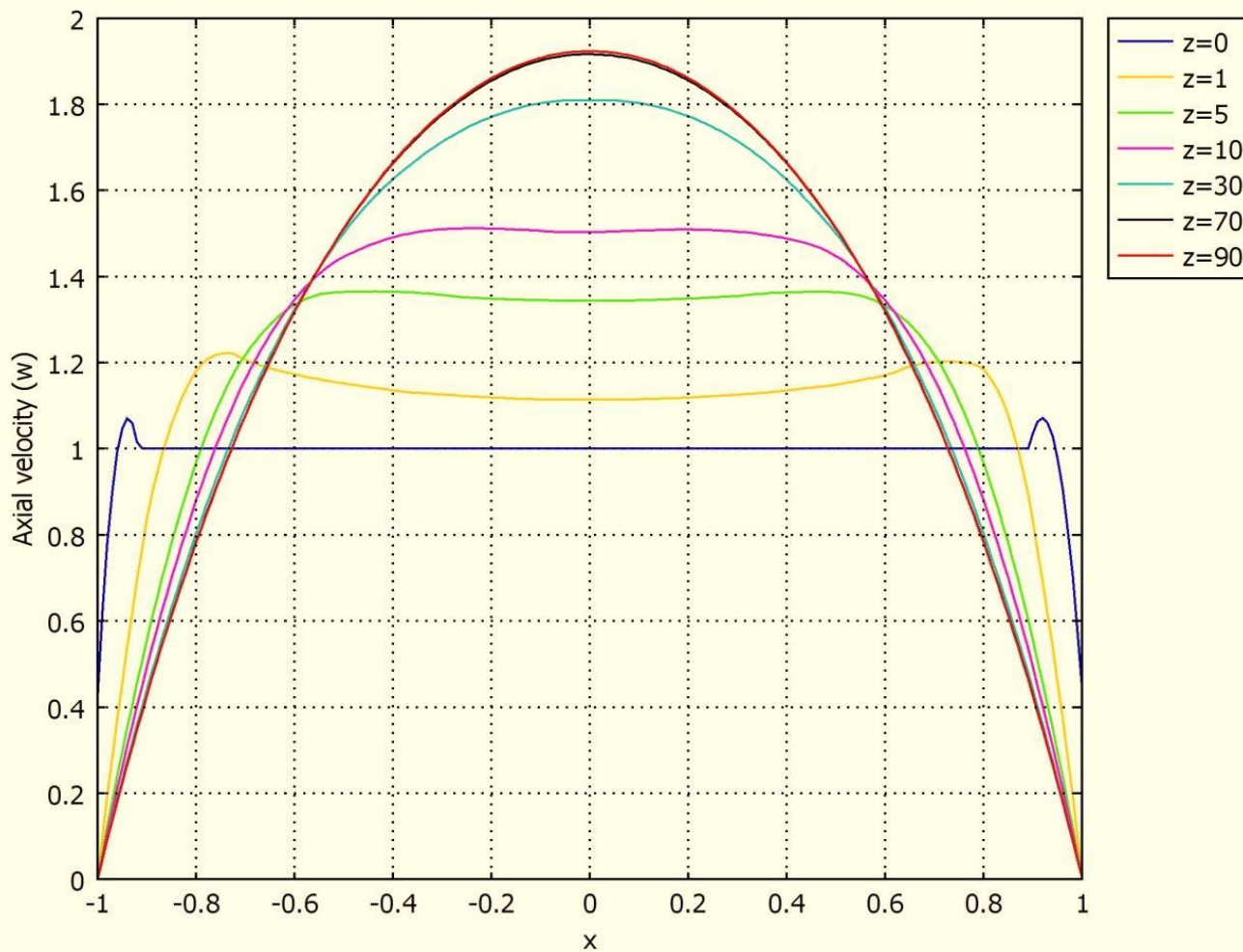
$$B_0 = 9Ha$$



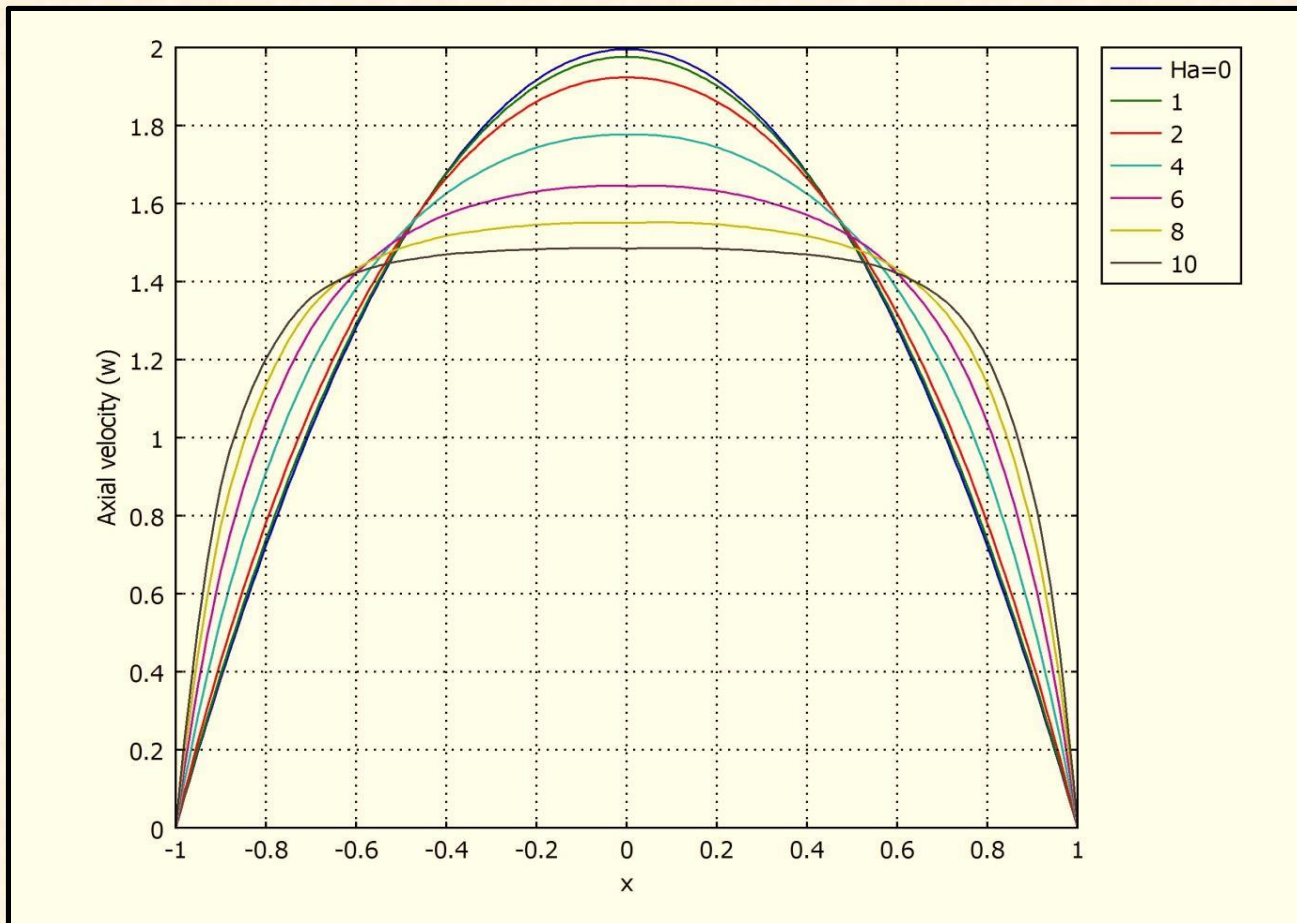
Comparison of axial velocity profile in the developed flow region with the analytical solutions obtained by Fabri & Siestrunk (1960) for $Ha=1$ and 10.

Fabri J and Siestrunk R, Contribution a la theorie aerodynamique du debitmetre electromagnetique”, *Bull. Assoc. Tech. Maritime Aeronautique.*, 1960: **60; 333-350.**

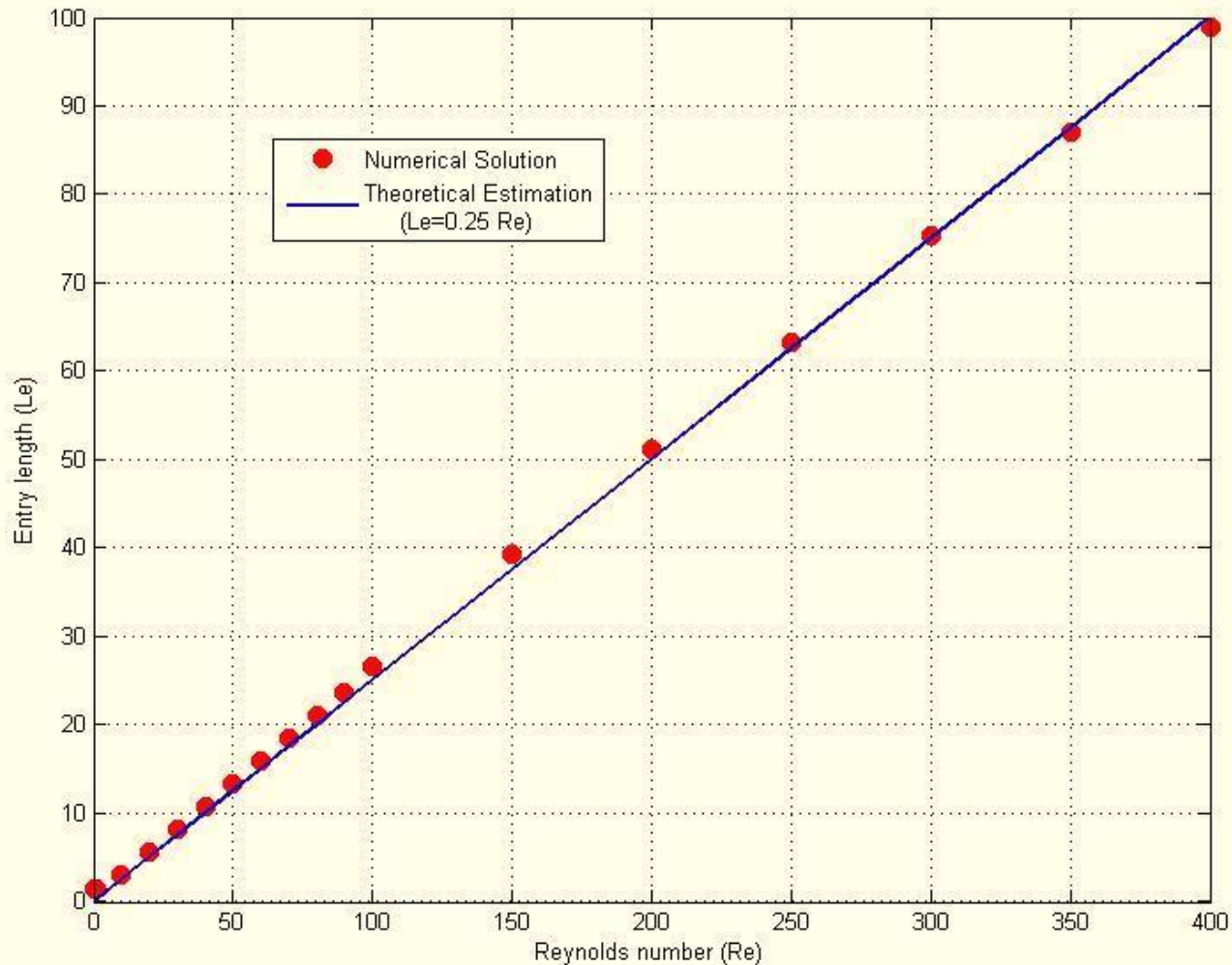
Excerpt from the Proceedings of the 2014 COMSOL Conference in Bangalore



Steady flow development of axial velocity at different axial position along the tube, $Re=300$, $Ha=2$

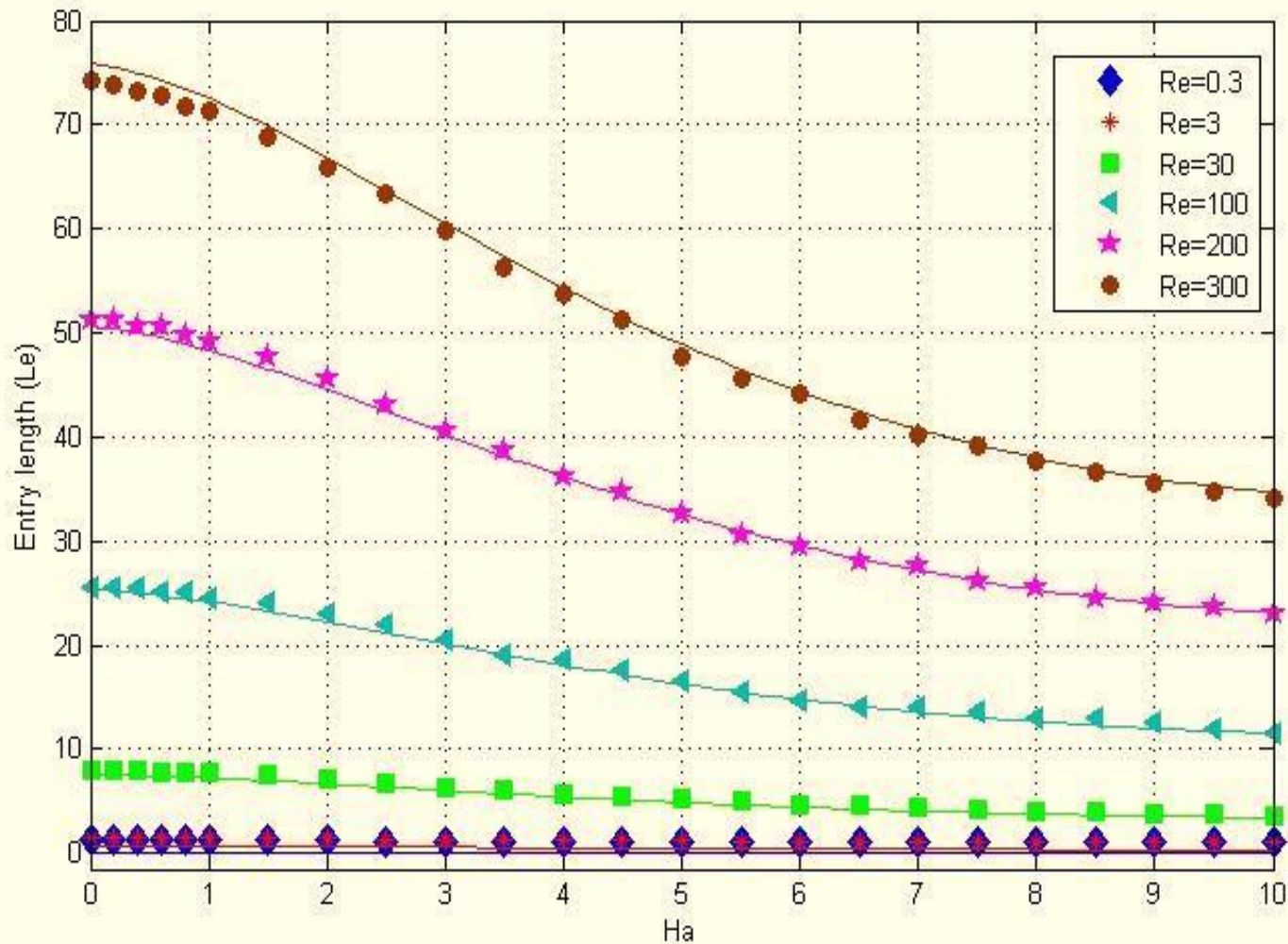


Axial velocity profile for different values of the Hartmann number Ha , when the flow is fully-developed with $Re=300$



Entrance length for steady case with different Reynolds number without applying magnetic field ($Ha=0$)

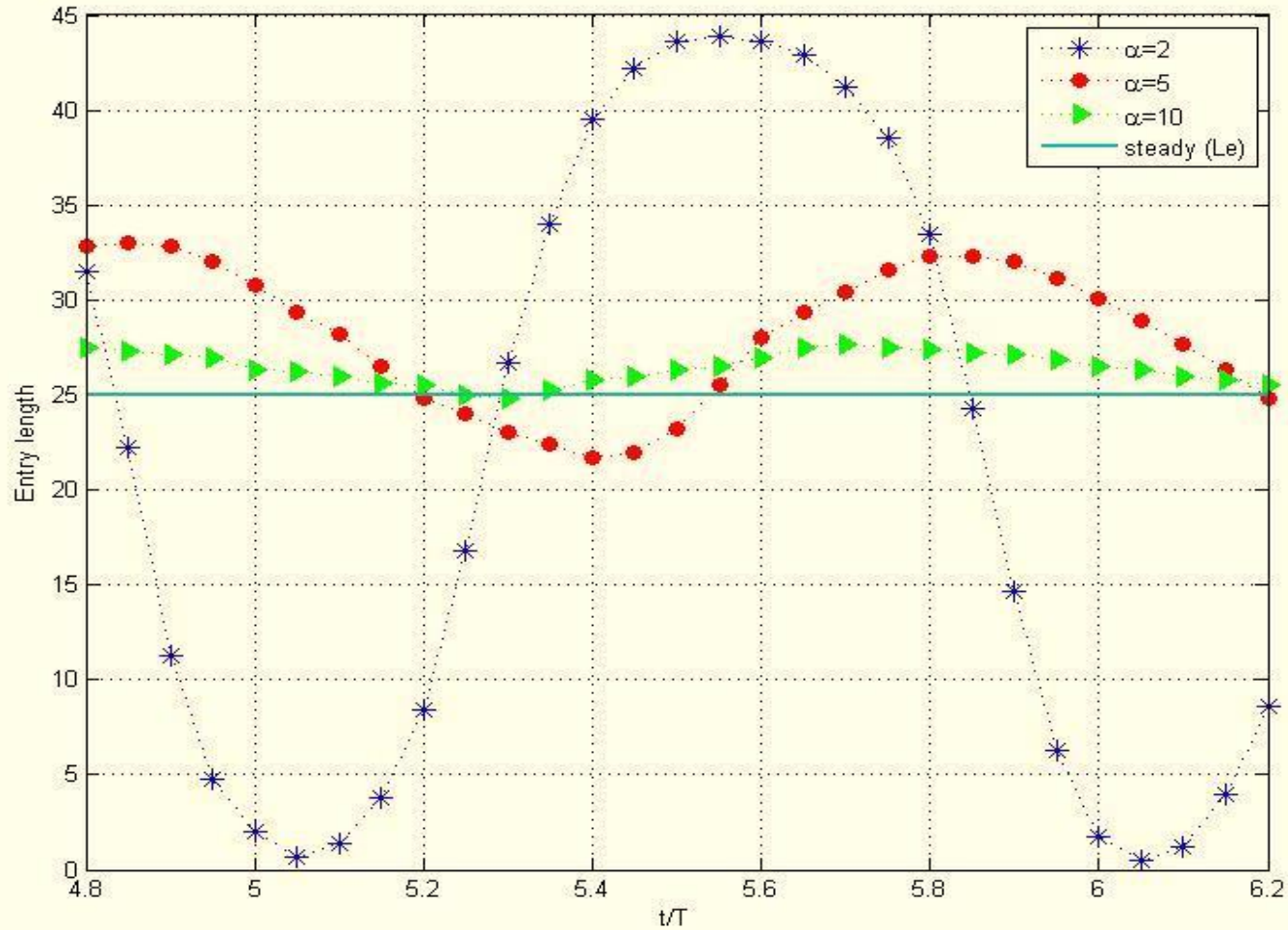
Excerpt from the Proceedings of the 2014 COMSOL Conference in Bangalore



Steady entrance length with Hartmann number Ha .

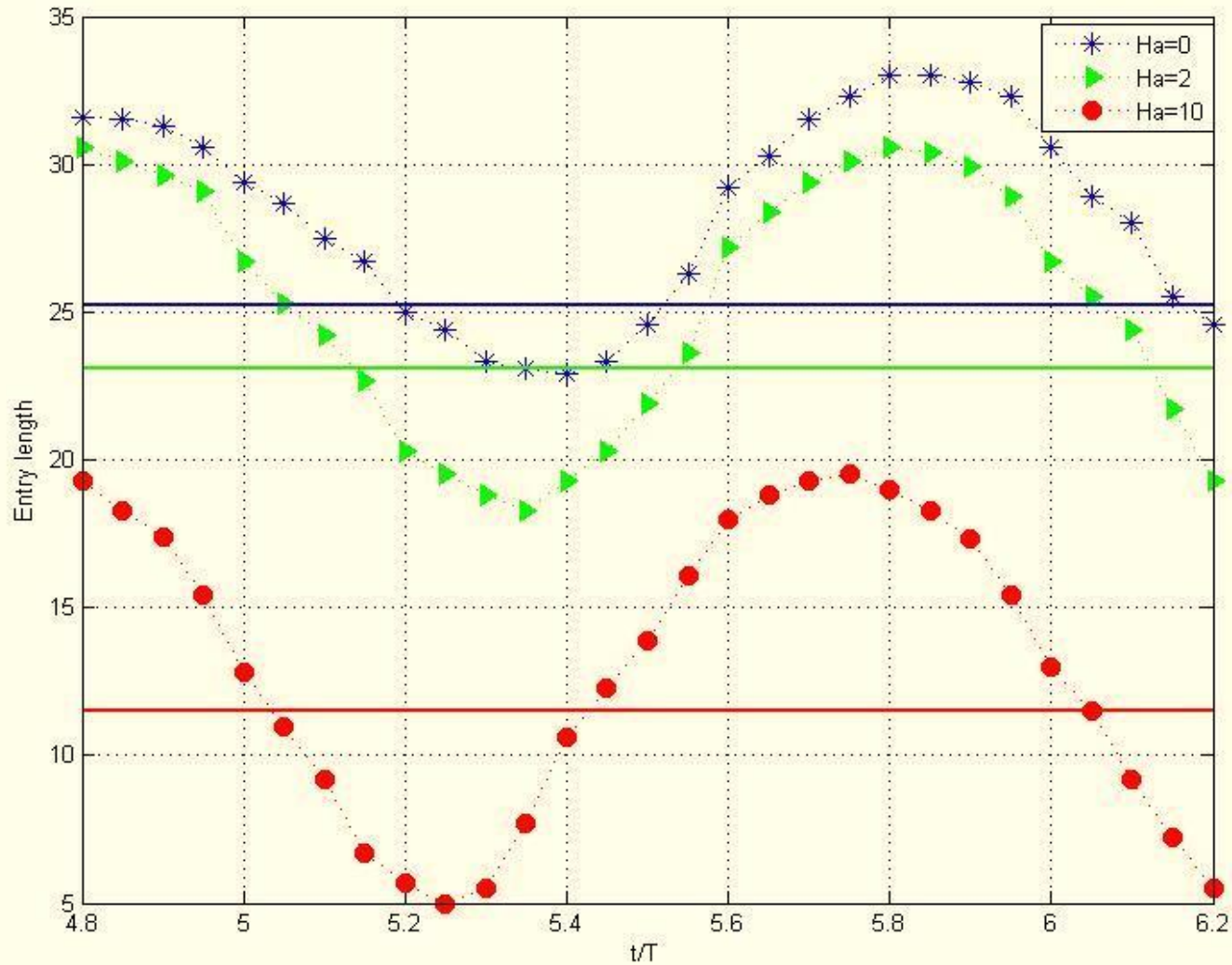
$$Le \cong \frac{0.25 Re}{1 + 0.024 Ha + 0.025 Ha^2 - 0.0016 Ha^3}$$

Excerpt from the Proceedings of the 2014 COMSOL Conference in Bangalore



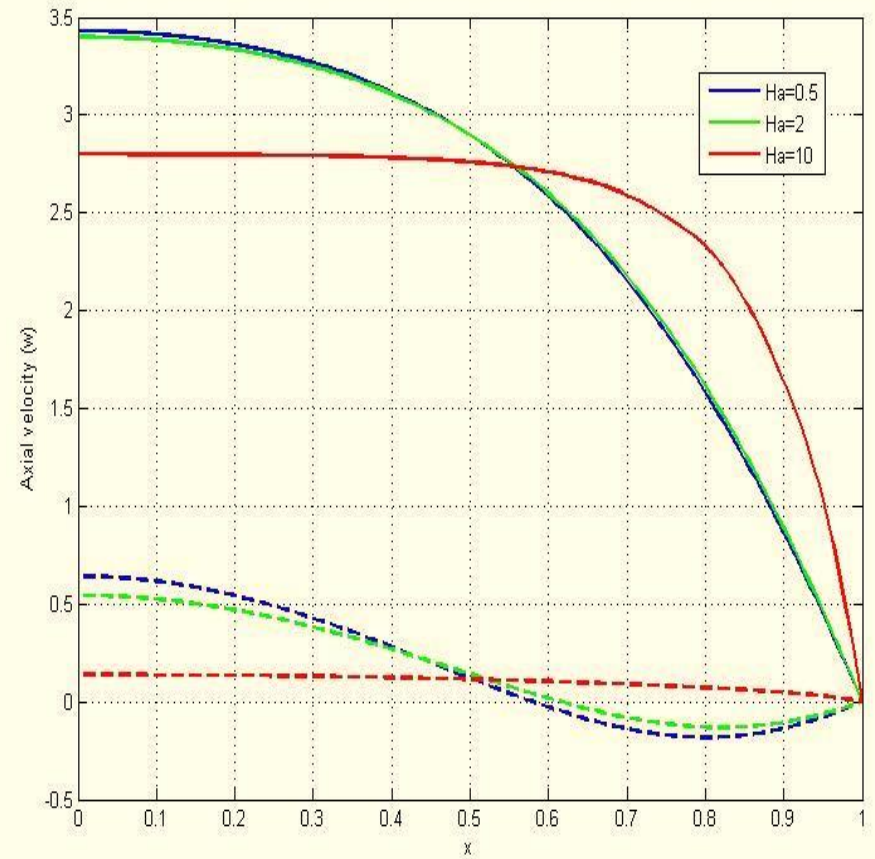
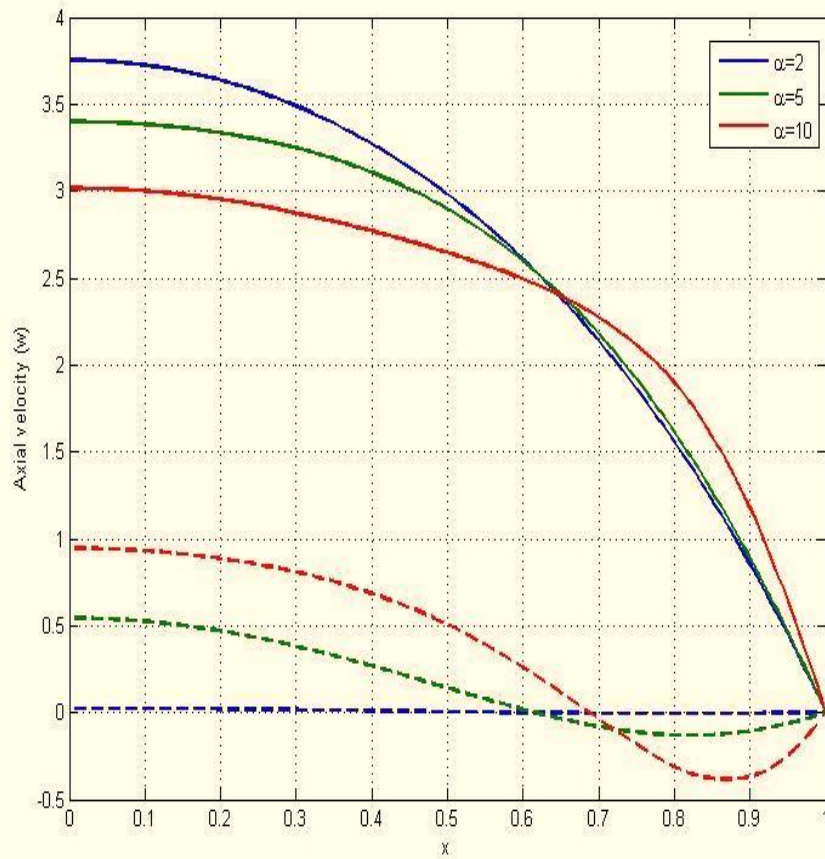
Unsteady entrance length with time for different Womersley parameter, when $Re=100$, $Ha=0.5$

Excerpt from the Proceedings of the 2014 COMSOL Conference in Bangalore

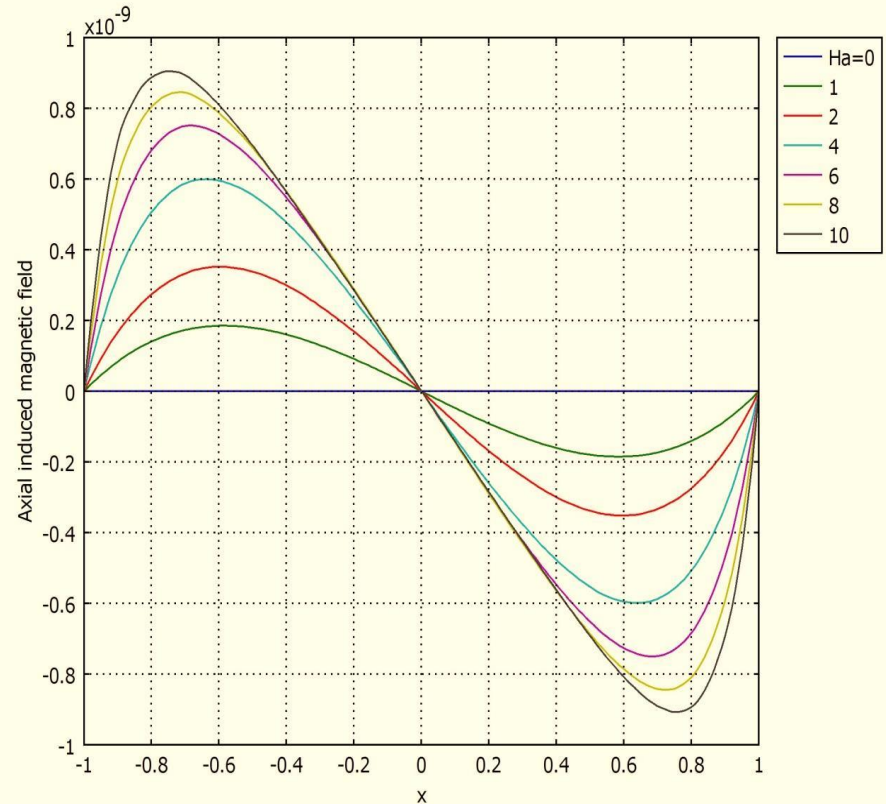
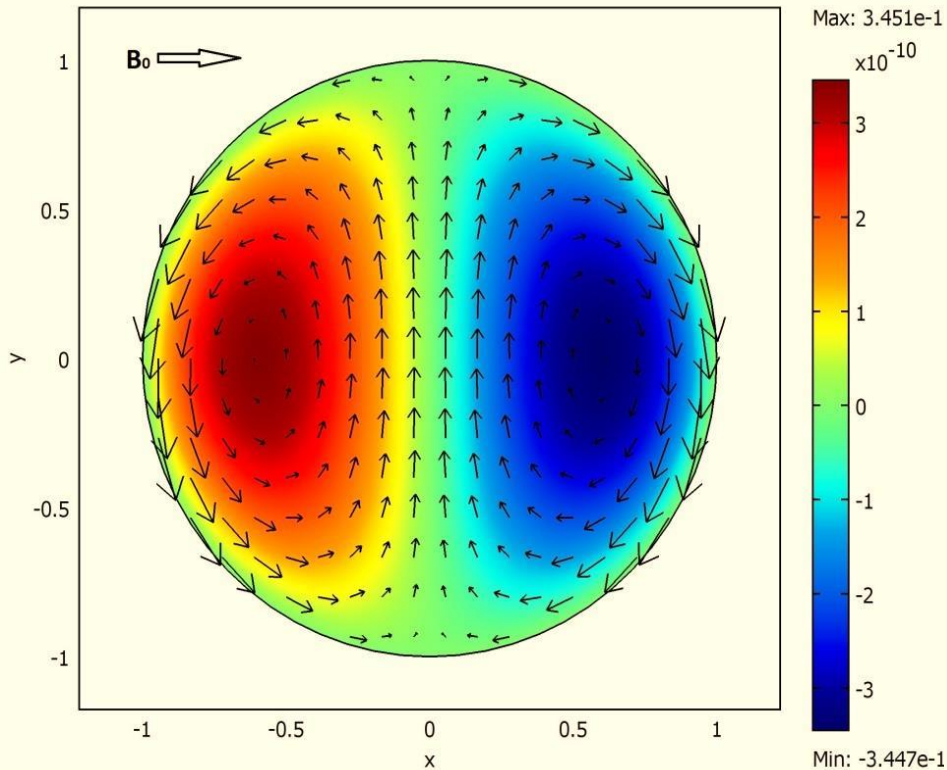


Unsteady entrance length with time for different Hartmann number Ha , when $Re=100$, $\alpha = 5$

Excerpt from the Proceedings of the 2014 COMSOL Conference in Bangalore

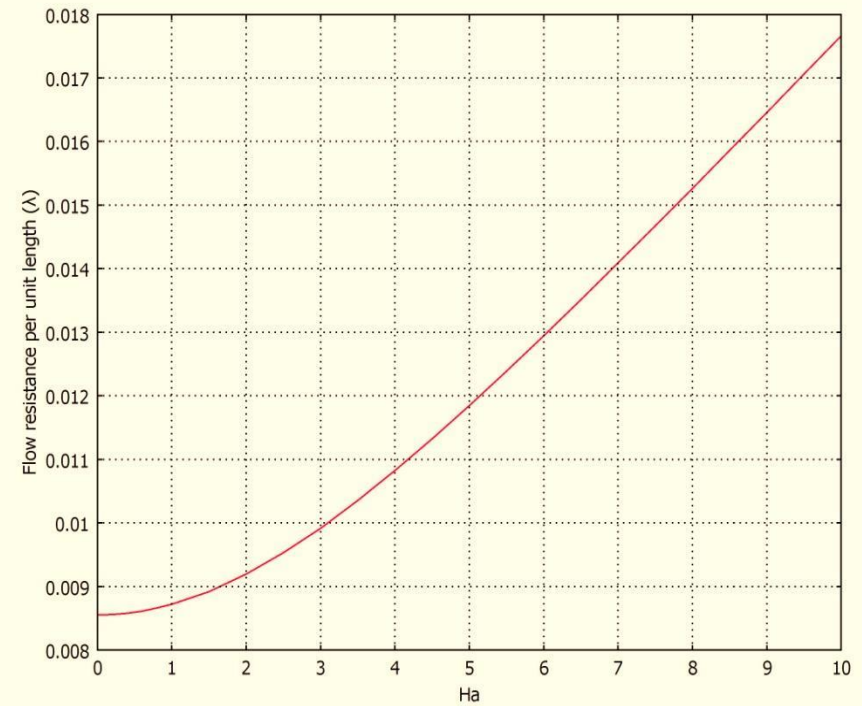
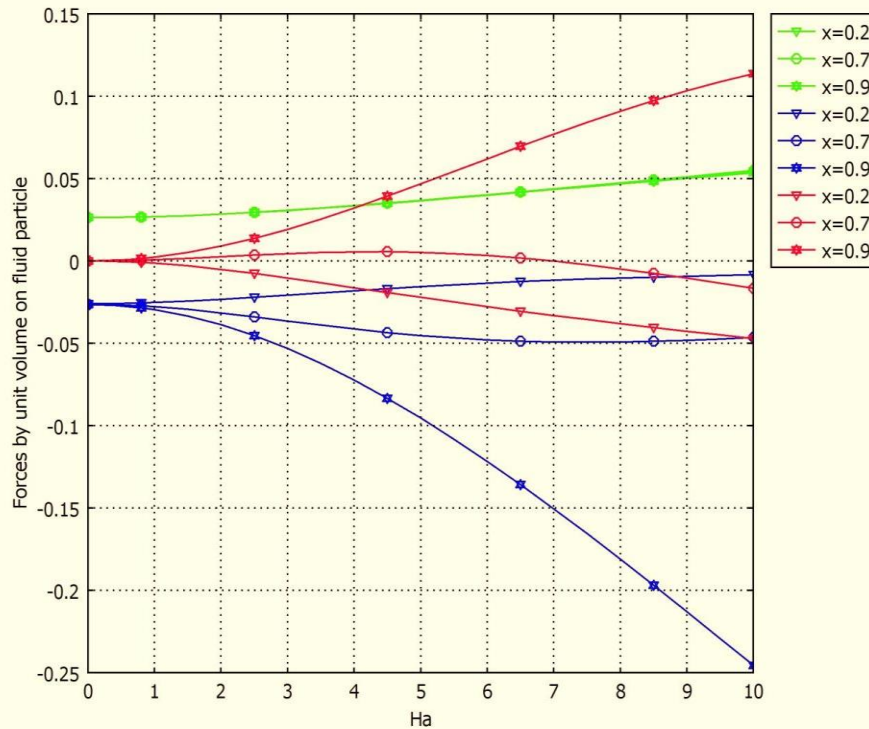


Axial velocity profiles at the peak (solid) lines and at the minimal (dotted) lines for different values of the Womersley parameter (left) and for different Hartmann number Ha (right)



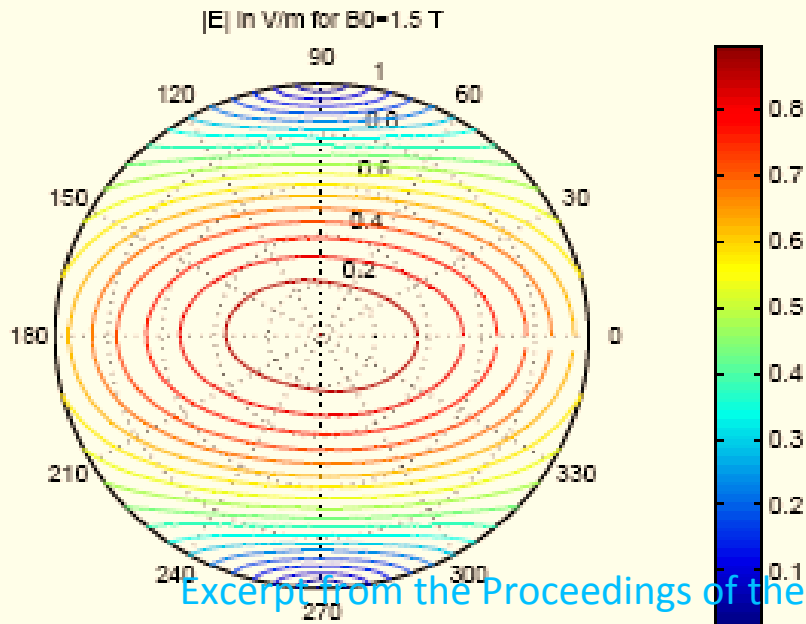
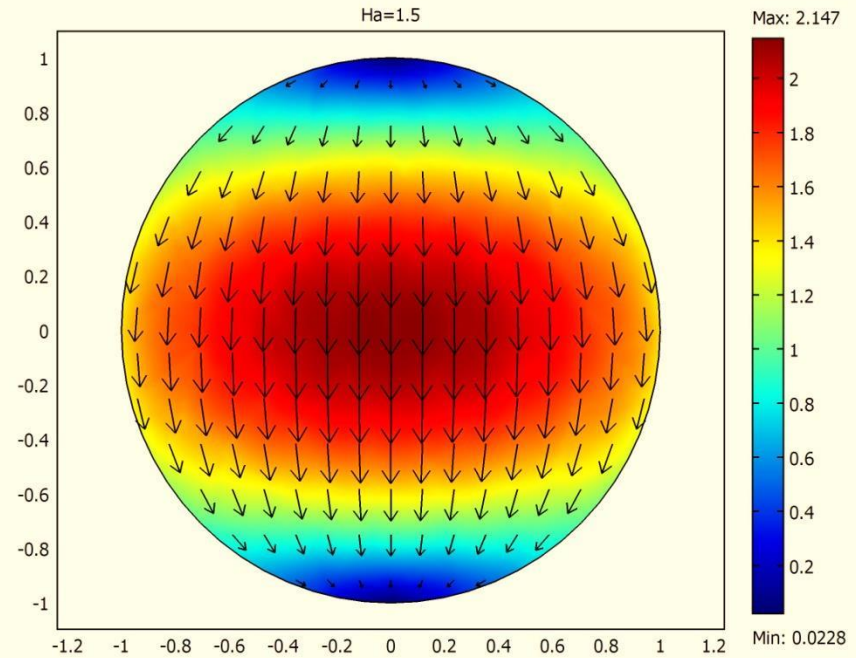
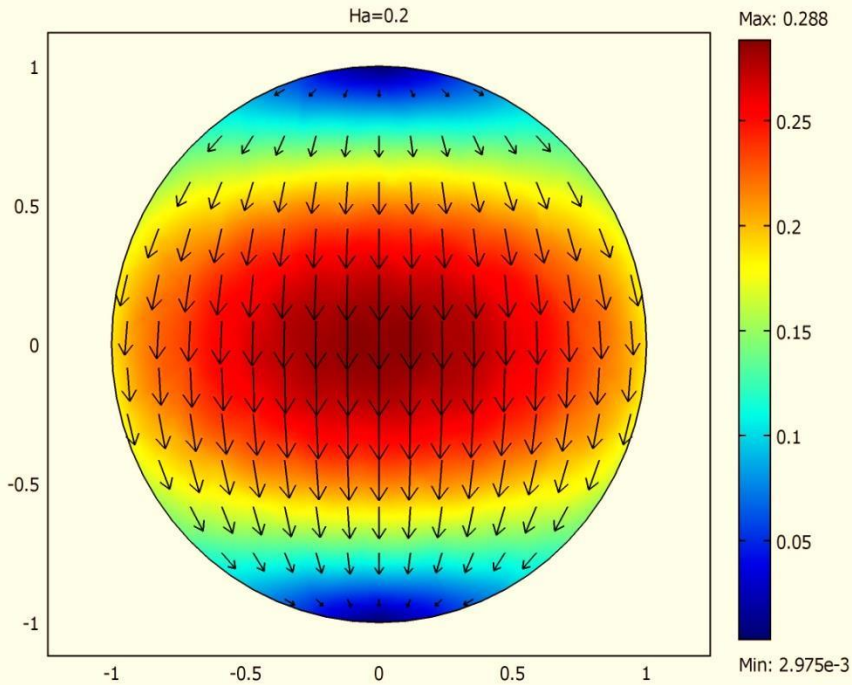
Plot with colour represents the axial induced magnetic field and arrow plot indicates the induced current density in steady case for $Re=300$, $Ha=2$

Variation of axial induced magnetic field for different Hartmann number Ha in steady case for $Re=300$



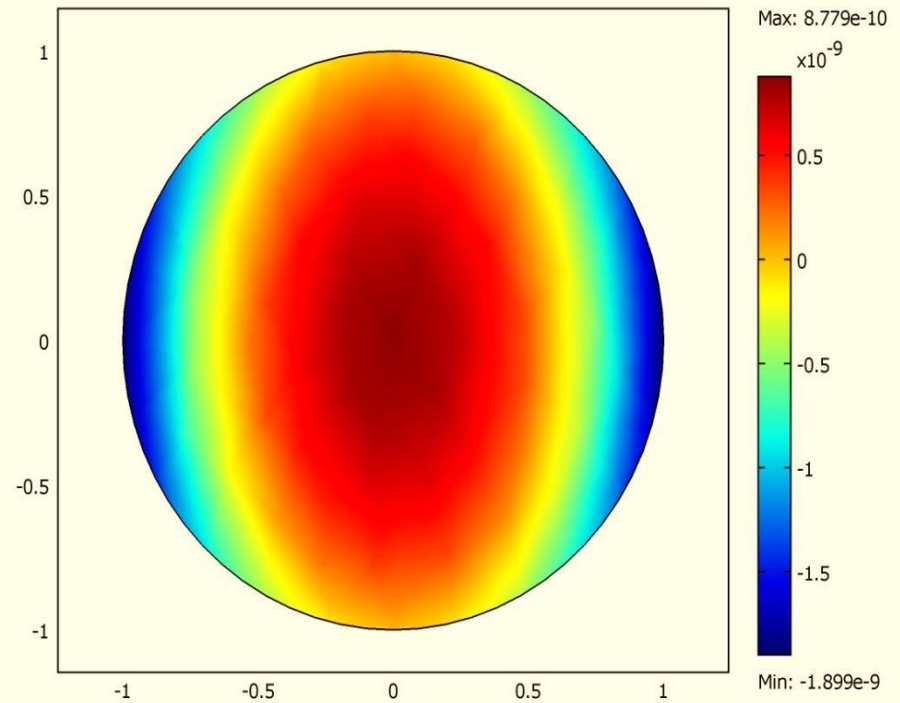
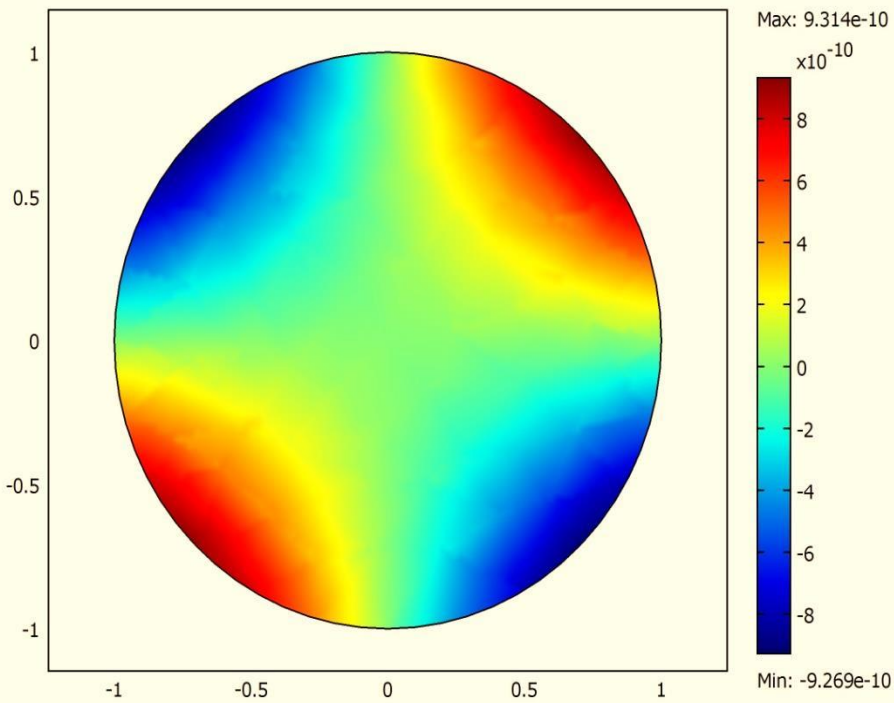
Variation of different forces by unit volume on the fluid particle (pressure gradient force indicated by green colour, Viscous forces indicated by blue colour and Magnetic forces by red colour) with Hartmann Ha, in steady case for Re=300

Variation of flow resistance per unit length ($\lambda = \frac{-\Delta p / \Delta z}{Q}$) with Hartmann number Ha for Re=300

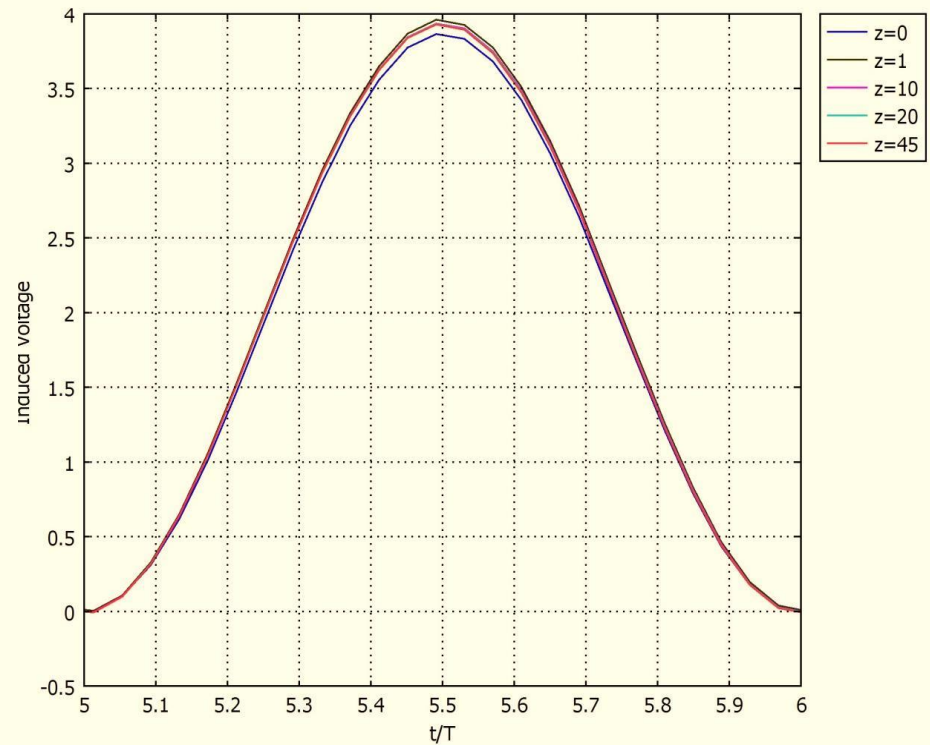
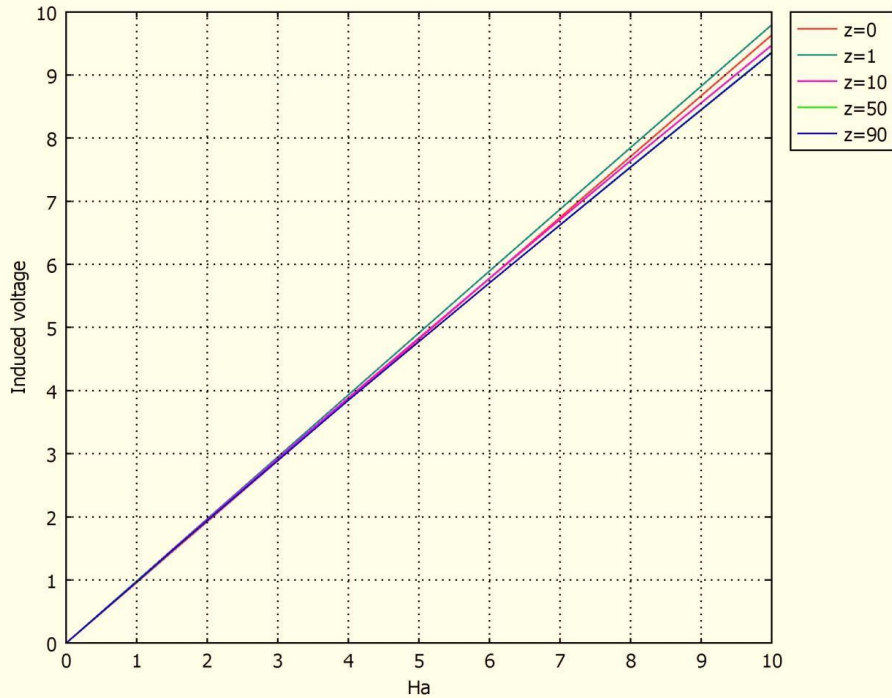


Plot shown in colour is the magnitude of the electric field and arrow plots indicate the direction of induced electric field,

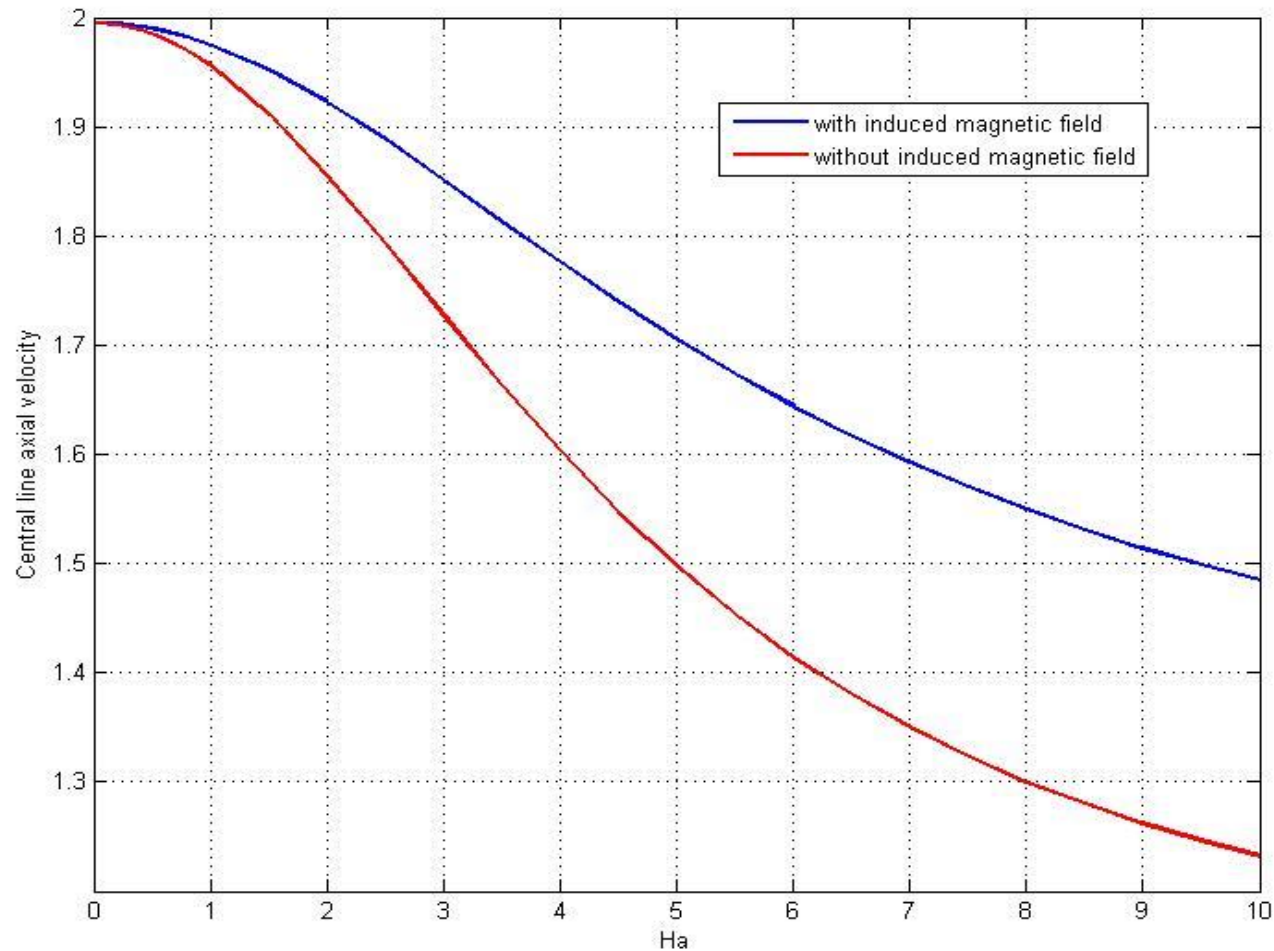
$$\vec{E} = \frac{1}{R\omega} \vec{\nabla} \times \vec{b} - \vec{\nabla} \times (Ha\hat{i} + \vec{b})$$



Non-dimensional amplitude of the current density components J_x and J_y for $Ha=1$ and $Ha=3$ respectively.



Effect of steady and unsteady entrance length on induced voltage with Ha and time respectively for $Ha = 2$, $Re = 100$, $\alpha = 5$



Reduction in mean velocity with Hartmann number Ha

Excerpt from the Proceedings of the 2014 COMSOL Conference in Bangalore

Conclusions

- The steady entrance length is found to be increase with Reynolds number Re and decrease with the increase of Hartmann number Ha . The steady entrance length in terms of magnetic field strength can be approximated theoretically as shown earlier.
- The sinusoidal variation with time in cycle is observed for unsteady entrance length. The unsteady entrance length is also decreases with Hartmann number Ha . The phase difference is observed in unsteady entrance length for the presence of both the parameters α and Ha
- During pulsatile blood flow, the reverse flow can be strongly suppressed by applying strong magnetic field. The Womersley parameter has reducing effect on flow velocity in the core region and an enhancing effect in the boundary layer during its peak flow, while the trend is reversed in the case of minimal flow rate.

- The interaction between induced currents and applied magnetic field causes reduction in flow velocity and thereby increases blood pressure in order to retain constant flow rate. The induced magnetic field forms two lobes on each side of the main current line and the induced currents re-circulates inside the vessel, due to the consideration of non-conducting vessel walls. **Thus the effect of induced magnetic field should not be overcome.**
- The induced voltage also varying sinusoidally with time and proportional to the applied magnetic field only. **It is worth mentioning here that the induced voltage does not depend on the development of flow field.**
- We may also conclude that finding **analytical solutions with the interaction of electromagnetic field in unsteady case is not possible and thus the numerical simulation is the only way of its solution**

References

1. G. C. Shit, Computational modeling of blood flow development and its characteristics in magnetic environment, ***Modelling and Simulation in Engineering (Hindawi)***, 2013: **2013**; Article ID: 758748, 12 pages.
2. G. C. Shit, M. Roy and Y. K. Ng: Effect of induced magnetic field on Peristaltic flow of a micropolar fluid in an asymmetric channel, ***International Journal for Numerical Methods in Biomedical Engineering (Wiley Interscience)***, 2010: **26**; 1380-1403.
3. R. R. Gold, “Magnetohydrodynamics pipe flow, Part-I”, ***Journal of Fluid Mechanics***, 1962: **13**; 505-512.
4. Abi-Abdallah D, Drochon A, Robin Vand Fokapu O, “Effects of static magnetic field exposure on blood flow”, ***The European Physical Journal: Applied Physics***, 2009: **45**; 11301.
5. X. He and D. N. Ku, “Unsteady entrance flow development in a straight tube”, ***ASME Journal of Biomechanical Engineering***, 1994: **116**; 355-360.

Thank you all for your kind
attention